



Published in final edited form as:

Osteoarthritis Cartilage. 2019 October ; 27(10): 1526–1536. doi:10.1016/j.joca.2019.06.005.

Low-level cyclic tibial compression attenuates early osteoarthritis progression after joint injury in mice

Derek T. Holyoak, MS¹, Carolyn Chlebek, BS¹, Matthew J. Kim¹, Timothy M. Wright, PhD^{1,2,3}, Miguel Otero, PhD², Marjolein C.H. van der Meulen, PhD^{1,2}

¹Cornell University, Ithaca, NY

²Hospital for Special Surgery, New York, NY

³Weill Cornell Medicine, New York, NY

Abstract

Objective: Mechanical loading and joint health have a unique relationship in osteoarthritis (OA) onset and progression. Although high load levels adversely affect cartilage health, exercise that involves low to moderate load levels can alleviate OA symptoms. We sought to isolate the beneficial effects of mechanical loading using controlled *in vivo* cyclic tibial compression. We hypothesized that low-level cyclic compression would attenuate post-traumatic OA symptoms induced by destabilization of the medial meniscus (DMM).

Methods: Ten-week-old C57B1/6J male mice underwent DMM surgery (n=51). After a 5-day post-operative recovery period, we applied daily cyclic tibial compression to the operated limbs at low (1.0N or 2.0N) or moderate (4.5N) magnitudes for 2 or 6 weeks. At the completion of loading, we compared cartilage and peri-articular bone features of mice that underwent DMM and loading to mice that only underwent DMM.

Results: Compared to DMM alone, low-level cyclic compression for 6 weeks attenuated DMM-induced cartilage degradation (OARSI score, p=0.008, 95% CI: 0.093 to 0.949). Low-level loading attenuated DMM-induced osteophyte formation after 2 weeks (osteophyte size, p=0.033, 95% CL 3.27 to 114.45 μ m), and moderate loading attenuated subchondral bone sclerosis after 6 weeks (tissue mineral density, p=0.011, 95% CI: 6.32 to 70.60 mg HA/ccm) compared to limbs that only

Corresponding Author: Marjolein C.H. van der Meulen, Meinig School of Biomedical Engineering, Cornell University, 113 Weill Hall, Ithaca, NY 14853, Tel: (607) 255-1445, Fax: (607) 255-1222, mcv3@cornell.edu.

Author contributions

Conception and design of the study: DH, TW, MO, MVDM

Acquisition of data: DH, CC, MK

Analysis and interpretation of data: DH, CC, TW, MO, MVDM

Drafting of the article: DH, MVDM

Critical revision of the article for important intellectual content: DH, CC, MK, TW, MO, MVDM

Final approval of the article: DH, CC, MK, TW, MO, MVDM

Derek Holyoak (dth72@cornell.edu) and Marjolein van der Meulen (mcv3@cornell.edu) take responsibility for the integrity of the work as a whole, from inception to finished article.

Publisher's Disclaimer: This is a PDF file of an unedited manuscript that has been accepted for publication. As a service to our customers we are providing this early version of the manuscript. The manuscript will undergo copyediting, typesetting, and review of the resulting proof before it is published in its final citable form. Please note that during the production process errors may be discovered which could affect the content, and all legal disclaimers that apply to the journal pertain.

underwent DMM. Finally, loading had subtle beneficial effects on cartilage cellularity and aggrecanase activity after DMM.

Conclusion: Low-level cyclic compression is beneficial to joint health after an injury. Therefore, the progression of early OA may be attenuated by applying well controlled, low-level loading shortly following joint trauma.

Keywords

animal models; mechanical loading; post-traumatic osteoarthritis; non-invasive therapy; cartilage; osteophyte

Introduction

Osteoarthritis (OA) is a degenerative joint disease that affects millions of individuals and is the leading cause of disability in the elderly population¹⁻⁴. The three hallmarks of the end-stage disease are cartilage degradation, osteophyte formation, and subchondral bone sclerosis. During the OA process, chondrocytes undergo apoptosis⁵, and collagenases and aggrecanases degrade the cartilage matrix^{6,7}. Post-traumatic osteoarthritis (PTOA) is a subset of OA associated with joint injury and instability due to mechanical trauma⁸. Individuals who experience a joint injury, such as anterior cruciate ligament (ACL) rupture or meniscal tear, are at risk for developing PTOA due to altered joint kinematics and any trauma directly to the cartilage or adjacent bone^{9,10}. Providing interventions following joint injury may be beneficial to attenuate PTOA.

Mechanical loading, exercise, and joint health have a unique relationship in OA onset and progression. Excessive mechanical loading is a primary risk factor for OA¹¹. Loading at high levels can decrease aggrecan synthesis and induce chondrocyte apoptosis^{12,13}. Furthermore, high loads can rupture stabilizing ligaments or damage joint tissue, such as the meniscus or cartilage¹⁴. Conversely, mild exercise is a recommended intervention for early-stage OA¹⁵. Mild exercise involving low-level loading can increase aggrecan synthesis *in vitro* and maintain thicker cartilage *in vivo*^{16,17}. In rodents, treadmill running slowed the progression of injury-induced cartilage degradation¹⁸. Although low-level mechanical loading has potential to attenuate OA¹⁶⁻¹⁹, most experiments investigating the effects of beneficial loading have been either *in vitro* or involved exercise. *In vitro* studies using cartilage explants and/or chondrocyte culture do not recapitulate the response of the entire joint^{12,20}. In addition, exercise leads to systemic effects, including peri-articular muscular strengthening, improvements in proprioception, and weight reduction^{21,22}. These multiple effects obscure the contribution of factors that specifically benefit the joint²². Here, we sought to isolate the beneficial effects of low-level loading using *in vivo* cyclic tibial compression.

To date, *in vivo* cyclic tibial compression has been an effective approach to study the initiation and progression of load-induced OA^{14,23,24}. Cyclic compression at moderate (4.5N) and high (9.0N) load magnitudes induced OA-like pathology, including cartilage degradation, osteophyte formation, and subchondral bone changes, in young (10-week) and adult (26-week) mice²³⁻²⁶. This same approach has the potential to benefit cartilage health

at lower load levels that occur during normal gait²⁷. Thus, we sought to determine whether daily cyclic compression at low load magnitudes (1.0N and 2.0N) would attenuate PTOA. To accomplish this objective, we used low-level cyclic compression combined with surgically-induced PTOA, using the destabilization of the medial meniscus (DMM) model. DMM-operated limbs maintain normal kinematics during tibial loading, whereas joint subluxation occurs with ACL transection, another PTOA model²⁹. Following DMM and loading, we assessed tissue-level changes in the cartilage, peri-articular bone, and menisci. In addition, we analyzed chondrocyte apoptosis, aggrecanase activity, and surface collagen loss. We hypothesized that cyclic compression at low load magnitudes would attenuate DMM-induced PTOA.

Methods

Animals

We used 10-week-old male C57BL/6J mice (n=51, The Jackson Laboratory, Bar Harbor, ME, USA). DMM surgery in 10-week old male mice leads to a robust, time-dependent progression of the disease^{24,28,30}. 3–5 mice were housed per cage. Lighting was maintained at a 12-hours-on-12-hours-off schedule. Food and water were provided *ad libitum*. All experimental techniques were approved by the Cornell IACUC and followed ARRIVE guidelines³¹. Briefly, animals underwent DMM surgery²⁸. Starting at five days after surgery, cyclic tibial compression was applied to the operated limbs for either 2 or 6 weeks. Upon completion of loading, knee joints were analyzed by histology, immunohistochemistry, and morphology.

DMM surgeries

We performed DMM surgery on the right knee joints of all mice²⁸. A 3mm skin incision was made with a #15 blade to expose the patellar tendon. Then a soft tissue incision was made directly medial to the patellar tendon from the distal patella to the proximal tibial plateau. While the patellar tendon was pulled laterally with a Tyrell Hook (without dislocating the patella), the fat pad was shifted laterally with a #11 scalpel blade until the medial meniscotibial ligament (MMTL) was exposed. Then, we positioned the scalpel blade inferior to the MMTL with the sharp edge facing laterally and rotated the blade clockwise until the MMTL ruptured. To verify each surgery, we translated the medial meniscus medially using the blunt edge of the scalpel. We closed the soft tissue and skin incisions with 6–0 and 7–0 prolene sutures, respectively (8706H, 8708H, Ethicon). Buprenorphine (0.1 mg/kg, Reckitt, VA) was administered immediately post-operatively, and once daily thereafter for 4 days.

Mechanical loading and experimental design

After a 5-day recovery period from DMM¹⁹, mice were randomized into seven groups (n=7–8/group) (Fig. 1). One group was euthanized immediately after the recovery period to investigate short-term damage caused by DMM (*DMM-only*: +0-weeks). Two groups were +2-week time points (following 5-day recovery period). For one +2-week group, cyclic compression was applied to DMM-operated tibiae at peak loads of 1.0N for 2 weeks (*DMM +1.0N*: +2-weeks). The second +2-week group received daily 5-minute doses of anesthesia without cyclic tibial compression (*DMM-only*: +2-weeks). The remaining four groups were

+6-week time points (following 5-day recovery period). For three +6-week groups, cyclic compression was applied to the DMM-operated right tibiae at 1.0N, 2.0N, or 4.5N peak loads for 6 weeks (*DMM+1.0N*, *DMM+2.0N*, *DMM+4.5N*: +6-weeks). The final +6-week group received daily anesthesia without tibial compression (*DMM-only*: +6-weeks).

For all loaded groups, the right limb received cyclic compression under general anesthesia (2% isoflurane, 1.0L/min, Webster) using a custom-made tibial loading device^{32–34}. Loading consisted of 1200 cycles/day at 4 Hz for 5 days/week. Load waveforms were triangular with load/unload ramps for 0.075 seconds each and dwell times of 0.100 seconds. Contralateral limbs served as controls. Mice were euthanized by CO₂ inhalation. Knee joints were harvested and fixed in 4% paraformaldehyde. After fixation, tissues were transferred to 70% ethanol for short-term storage for microcomputed tomography (microCT) prior to decalcification and sectioning.

Cartilage morphological changes

Knee joints were decalcified in EDTA and processed for paraffin embedding. Paraffin blocks were sectioned at a 6- μ m-thickness from posterior to anterior using a rotary microtome (Leica RM2255, Wetzlar, Germany). To assess cartilage morphology, sections were stained with Safranin-O/Fast Green at 90- μ m intervals. Histological OARSI scoring was performed blinded by two observers to examine structural cartilage damage in the medial tibial plateau³⁵. Average and maximum scores of each limb were calculated independently for each observer, and these scores were averaged over the two observers.

Osteophyte formation

We examined Safranin-O/Fast Green-stained histological sections for osteophyte formation. We analyzed osteophytes in the medial tibial plateau from three representative sections in the joint (anterior, middle, posterior). Osteophyte maturity was evaluated based on the degree of calcification of the ectopic bone³⁶. We also measured the medial-lateral width of the osteophyte, defined as the distance between the medial end of the epiphysis and the end of the osteophyte²⁵.

Peri-articular bone morphological changes

Bone architecture changes at the +6-week time point were determined by microCT. Prior to decalcification, intact knee joints were scanned by microCT with an isotropic voxel resolution of 10 μ m (μ CT35, Scanco, Bruttisellen, Switzerland; 55kVp, 145 μ A, 600ms integration time). We examined the subchondral bone plate (SBP) and cancellous bone in the epiphysis and metaphysis of the proximal tibia^{25,26}. SBP parameters included plate thickness and tissue mineral density (TMD). Cancellous bone parameters included bone volume fraction (BV/TV), trabecular thickness (Tb.Th), trabecular separation (Tb.Sp), and cancellous TMD.

Chondrocyte apoptosis

We assessed chondrocyte apoptosis after DMM surgery and 1.0N-loading using a TUNEL kit to detect DNA strand breaks (Sigma, 11684795910 Roche, Darmstadt, Germany). We stained representative sections from the middle region of each limb at all time points.

Sections were deparaffinized, rehydrated, and incubated with proteinase K at 37°C. Then, samples were incubated with the TUNEL reaction mixture for 1h at 37°C. Finally, sections were mounted using antifade medium containing DAPI. The total area of DAPI+ staining was measured in the articular cartilage of the medial tibial plateau (ImageJ software, NIH)^{37–38}. The DAPI+ signal was normalized to cartilage area. TUNEL+ staining was measured and normalized to the DAPI+ signal to account for cellularity.

Aggrecanase activity

Aggrecanase activity was assessed in a subset using immunohistochemistry (IHC). We stained representative sections from the middle region of control and DMM-operated limbs from animals in the *DMM-only* and *DMM+I. ON* groups at the +2-week and +6-week time points³⁹. Sections were deparaffinized, rehydrated, and incubated with a mild temperature retrieval solution at 60°C for 30min (UNI-TRIEVE, Innovex, Richmond, CA). Endogenous peroxidase activity was quenched for 15min at room temperature (RT) (PEROX-BLOCK, Innovex). Background staining was minimized for 30min at RT (Background Buster, Innovex). Newly generated aggrecanase-driven neopeptides on aggrecan were detected using an anti-NITEGE primary antibody (ThermoFisher PA-1–1746) with 1:100 ratio of immunodiluent for 2h at RT. Secondary linking antibody and horseradish peroxidase-enzyme (STAT Animal IHC Kit, Innovex) were used for 10min each at RT. Fresh DAB solution was applied for 5min at RT, and staining intensity was enhanced for 3min at RT (Quick DAB Enhancer, Innovex). Sections were washed with water and mounted (Advantage Mounting Medium, Innovex). The total area of positive immunostaining in the articular cartilage of the medial tibial plateau was calculated and normalized to cartilage area (ImageJ software, NIH)^{37,38}.

Surface collagen content

We assessed surface collagen content using picrosirius red staining. We stained representative sections from the middle region of each limb at all time points. Sections were deparaffinized, rehydrated, and incubated with 0.1% Direct Red 80 (Sigma-Aldrich, 365548) in saturated picric acid for 60min at RT, followed by dehydration and mounting. Using custom software (MATLAB, Math Works), the number of positively stained pixels in the cartilage surface was counted and normalized to the total number of pixels in the surface.

Synovitis

Synovitis was evaluated in representative anterior, middle, and posterior sections at +6-weeks. Enlargement of the cell layer and cell density were individually evaluated⁴⁰.

Meniscal ossicle morphology

Anterior meniscal ossicle morphology was characterized using microCT. The VOI included all positive signal in the medial joint space, excluding the fabella. We assessed meniscus volume and density⁴¹.

Statistical analyses

For histological evaluations, we compared limbs across groups at +6-weeks using a one-way ANOVA with animal as a random effect. Parameters analyzed by one-way ANOVA included OARSI scores, osteophytes, cellularity, apoptosis, aggrecanase activity, surface collagen content, and synovitis. OARSI scores, osteophytes, aggrecanase activity, and surface collagen content from DMM-only and DMM+1.0N groups were examined across timepoints of +0, +2, and +6-weeks using a two-way ANOVA with group and timepoint as variables, and animal as a random effect. Contralateral limbs from the *DMM-only* group were used as controls for histology. Subchondral bone plate, cancellous bone, and meniscal ossicle measurements from microCT at +6-weeks were analyzed using a two-way ANOVA with limb and group as variables and animal as a random effect. Normality was confirmed visually using histograms and QQ plots of the residuals. Homogenous variance was assessed visually using plots of residuals against predicted values.

Results

Low-level cyclic compression attenuated DMM-induced cartilage degradation

After the 5-day recovery period post-DMM surgery (+0-weeks), cartilage damage was minimal (Fig. 2A,B,C). Mild localized proteoglycan loss occurred in some limbs, but neither average nor maximum OARSI scores were different from control limbs at +0-weeks. Two weeks after the 5-day recovery (+2-weeks), proteoglycan loss and mild erosion were present in *DMM-only* limbs. In the *DMM+LON* group at +2-weeks, moderate proteoglycan loss was visible in the cartilage. At the +6-week time point, severe cartilage erosion occurred in *DMM-only* limbs. In the *DMM+1.0N* group at +6-weeks, the cartilage surface was generally intact, and structural changes were limited to focal proteoglycan loss. At +6-weeks, average, but not maximum, OARSI scores in the *DMM+1.0N* group were significantly lower than scores from the *DMM-only* limbs (Table S-1).

Cyclic compression at 2.0N had similar effects to 1.0N-loading at +6-weeks (Fig. 2A,D,E). The cartilage surface from 2.0N-loaded limbs was generally intact, but proteoglycan loss was evident. At +6-weeks, average OARSI scores were significantly lower in the *DMM+2.0N* group compared to the *DMM-only* group. Loading at 4.5N led to moderate cartilage erosion and proteoglycan loss. At +6-weeks, OARSI scores were not significantly different between the *DMM-only* and *DMM+4.5N* groups.

Low-level cyclic compression attenuated DMM-induced osteophyte formation

Low-level tibial compression attenuated early osteophyte growth on the posteromedial aspect of the tibial plateau (Fig. 3). Posteromedial osteophytes formed in the *DMM-only* groups at all time points. Growth was attenuated with 1.0N-loading at +2-weeks, but not at +6-weeks. (Fig. 3A,B). In addition, osteophyte maturity at +6-weeks was lower in the *DMM+1.0N* group compared to the *DMM-only* group (Table S-2).

On the anterior portion of the tibial plateau, medial osteophyte size increased after the 5-day recovery period in the *DMM-only* group (+0-weeks) compared to controls (Fig. 3C,D). Anteromedial osteophyte size continued to increase in the *DMM-only* and *DMM+1.0N*

groups after 2 and 6 weeks. Anteromedial osteophyte maturity was not different between *DMM-only* and *DMM+1.0N* groups.

Loading attenuated DMM-induced subchondral bone sclerosis but not cancellous bone loss

At all load levels cyclic compression attenuated subchondral bone sclerosis after DMM surgery (Fig. 4, Table S-2). At +6-weeks, DMM led to a significant increase in TMD in the medial subchondral bone plate compared to control limbs in the *DMM-only* group (Fig. 4A). DMM surgery followed by 1.0N-, 2.0N-, or 4.5N-loading did not result in increased TMD in DMM-operated limbs compared to control limbs. However, TMD in *DMM-only* and DMM-loaded limbs was not different. Subchondral bone plate thickness was greater in the *DMM-only* group than the *DMM+4.5N* group (Fig. 4B).

At +6-weeks, cancellous bone volume fraction (BV/TV) in the epiphysis decreased in DMM-operated limbs compared to control limbs in all groups, regardless of whether the limbs underwent loading (Fig. S-1A). The decreased BV/TV was due to increased trabecular separation (Tb.Sp) following DMM (Fig. S-1B). Trabecular thickness (Tb.Th) was not different among any of the groups (Fig. S-1C). The *DMM-only* group had higher TMD compared to the three loaded groups (Fig. S-1D).

Similarly, bone loss occurred in the metaphysis at +6-weeks after DMM surgery, regardless of whether the limbs underwent loading (Fig. S-2A). Tb.Sp was greater in all DMM-operated limbs compared to control limbs (Fig. S-2B). DMM surgery did not induce any changes in metaphyseal Tb.Th (Fig. S-2C). Lastly, TMD was lower in all DMM-operated limbs compared to control limbs, regardless of whether the limbs underwent loading (Fig. S-2D).

Low-level loading had subtle beneficial effects on chondrocyte loss and apoptosis

Chondrocyte numbers decreased following DMM surgery, indicated by a loss of DAPI+ signal (Fig. 5A,B). At +0-weeks, cellularity was not different between *DMM-only* and control limbs. At +2-weeks, small localized areas of the cartilage had decreased cellularity in the *DMM-only* and *DMM+1.0N* groups. At +6-weeks, the *DMM-only* group had the least number of remaining cells with large portions of the tibial plateau lacking cellularity. DAPI+ stained cells in the +6-week *DMM-only* group were lower compared to the +2-week DMM-operated limbs. DAPI+ stained cells in the +6-week *DMM+1.0N* group were not significantly different from the +2-week groups but were lower than +6-week controls (Table S-1).

Subtle differences in chondrocyte apoptosis were evident among groups (Fig. 5A,C). Minimal apoptosis occurred in the +0-week *DMM-only* group. TUNEL+ staining increased slightly at +2-weeks in the *DMM-only* group but was not significantly different from +0-week levels. At +6-weeks, apoptosis levels in the *DMM-only* and *DMM+1.0N* groups were not different from each other and were higher compared to the +0-week timepoint. However, at +2-weeks, TUNEL+ staining in the *DMM-only* group was not different from +6-week levels, whereas the increase in TUNEL in the *DMM+1.0N* group was delayed.

Low-level loading had subtle beneficial effects on aggrecanase activity

NITEGE neopeptide levels in the *DMM-only* and *DMM+1.0N* were not significantly different from control limbs. However, *DMM-only* limbs had a mean increase of 116% in aggrecanase activity compared to control limbs, whereas *DMM+1.0N* limbs had an increase of 53% compared to control limbs. In addition, NITEGE neopeptide levels decreased by 59% from +2-weeks to +6-weeks (Fig. 6).

Loading had no effect on surface collagen content

Surface collagen content decreased with time in both *DMM-only* and *DMM+1.0N* groups (Fig. S-3). At +6-weeks, limbs from the *DMM-only* and *DMM+1.0N* groups had lower surface staining compared to the +0-week *DMM-only* group. However, picrosirius red staining between the *DMM-only* and *DMM+1.0N* groups was not different (Table S-1).

Synovitis scores did not change with DMM or loading

At +6-weeks, synovial changes (cellular density and synovial enlargement) were not different among control, *DMM-only*, and loaded limbs (Fig. S-4).

Loading had no effect on DMM-induced meniscal ossicle expansion

At +6-weeks, DMM surgery increased anteromedial meniscal ossicle volume compared to control limbs in all groups, regardless of whether the limbs underwent loading (Fig. S-5A,B). Meniscus volume in DMM-operated limbs was approximately 1.5x the volume of control limbs. In addition, meniscal ossicle density decreased after DMM surgery (Fig. S-5C).

Discussion

We examined whether non-invasive axial compression at low load magnitudes could attenuate PTOA progression following DMM. We hypothesized that low-level cyclic tibial compression would slow DMM-induced OA-like changes. After 6 weeks, limbs that underwent DMM surgery without additional loading had cartilage erosion extending to the tidemark, osteophytes on the medial tibial plateau, and sclerotic subchondral bone, consistent with previous studies²⁸. In addition, *DMM-only* limbs had decreased cellularity, loss of surface collagen, meniscal growth, cancellous bone loss, and a trend towards increased aggrecanase activity. Low-level cyclic compression initiated 5 days after DMM surgery attenuated many DMM-induced changes, including the hallmarks of OA: cartilage erosion, osteophyte formation, and subchondral bone sclerosis. Furthermore, low-level loading had subtle beneficial effects on cellularity, and a trend towards less aggrecanase activity compared to *DMM-only* limbs. However, loading did not attenuate cancellous bone loss, meniscal growth, or surface collagen loss. Overall, these results support our hypothesis that low-level cyclic compression can slow the progression of DMM-induced OA.

The effect of low-level cyclic tibial compression in the knee was opposite that of tibial compression at higher load magnitudes. Previously, cyclic tibial compression studies focused on the induction of OA-like damage following high levels of mechanical loading^{23,24}. Loading at 9.0N caused cartilage erosion, osteophyte formation, and

subchondral bone changes in both 10- and 26-week-old mice. Moderate loading at 4.5N caused mild cartilage surface degradation in 26-week-old mice, but minimal bone changes. In the current study, the 4.5N load level was expected to exacerbate DMM-induced OA progression in 10-week-old mice^{24,25}. However, the OA severity in the *DMM+4.5N* and *DMM-only* groups was not different; therefore, the 4.5N-load may be an intermediate level that is neither protective nor damaging in 10-week-old male mice. This outcome may reflect different effects of loading with a DMM-operated knee versus a healthy knee and with animal age. Low-level cyclic compression at 1.0N or 2.0N attenuated damaging effects from DMM surgery in 10-week-old mice. Overall, a dose response to load magnitude was evident. These results demonstrate the importance of load magnitude in the joint's response to tibial loading. In addition, the constant load/unload and dwell times across waveforms resulted in lower strain rates at lower load magnitudes. Strain rate is an independent parameter in the cartilage response to compression¹²; therefore, the lower strain rates during the lower-magnitude loading may also have promoted joint health.

The beneficial effects of cyclic axial compression were comparable to other noninvasive preclinical loading regimens. To our knowledge, the only beneficial reports of *in vivo* cyclic loading involved transverse loading of the knee in the medial-lateral direction at 1.0N for 2 weeks after surgical induction of OA in mice^{19,42,43}. Low-level transverse knee loading attenuated post-traumatic cartilage damage and bone mineral density changes. Therefore, low-level loading of the knee joint in both the medial-lateral and axial directions can attenuate cartilage and bone changes after injury. However, osteophyte formation has not been examined with transverse knee loading in the medial-lateral direction. In addition, transverse loading of the knee rarely occurs during activities of daily living, whereas axial joint loading occurs in most lower extremity exercises (i.e. walking, running, etc.). Thus, our findings support the direct beneficial effects of axial loading on articular cartilage during exercise.

Controlled, low-level loading was equally as effective, if not more effective, compared to preclinical exercise regimens used to benefit joint tissues. Activities involving mild to moderate mechanical loading of joints enhanced articular cartilage in multiple preclinical studies^{17,18,44,45}. Mice with lifelong access to running wheels maintained thicker cartilage compared to mice without running wheels¹⁷. In addition, low-intensity (30min/day) treadmill exercise attenuated cartilage degeneration in rats after DMM⁴⁴. However, gentle treadmill walking did not affect osteophyte formation after DMM⁴⁴, whereas low-level cyclic compression significantly attenuated DMM-induced posteromedial osteophyte formation in our study. The posterior region showed the most significant changes, most likely because during tibial loading the contact point occurs in the posterior region of the tibial plateau²⁹. Furthermore, the success of controlled loading following DMM in mice may reflect the lesser degree of joint instability associated with the DMM model compared to other ligament injury models²⁹. In destabilization models associated with increased joint laxity, such as ACL transection or rupture, *in vivo* loading may exacerbate joint instability and produce extreme kinematics. Nonetheless, although exercise is beneficial to articular cartilage, low-level cyclic compression resulted in additional benefits to joint tissues following DMM, possibly due to the controlled nature of the loading protocol.

The cartilage response to mechanical loading at the cellular and protein levels depends on load-induced strain levels⁴⁶. Low-level cyclic compression likely resulted in a beneficial response due to healthy tissue strains. The applied load was equal to 3–4x body weight, similar to loads applied during normal gait²⁷. In turn, these dynamic physiologic strains may have induced anabolic, anti-catabolic, or anti-inflammatory effects⁴⁶, attenuating PTOA. Therefore, we expected beneficial effects from loading at the cellular and protein levels. Based on our TUNEL data, low-level loading had subtle protective effects on cellularity and apoptosis. In addition, although significance was not observed due to small sample size, increases in aggrecanase activity were approximately double in *DMM-only* limbs compared to *DMM+1.0N* limbs. The surface collagen content was not retained with 1.0N-loading, but more intact cartilage tissue remained in the *DMM+1.0N* groups compared to the *DMM-only* groups. Further investigation of the mechanisms at the cellular and molecular levels will elucidate the beneficial effects of low-level cyclic strain on joint health.

The translation of these findings from mice to humans is important. Although cartilage strain levels during static murine tibial compression have been approximated using computational models⁴⁷, stresses and strains resulting from dynamic cyclic compression should be quantified. Clinically, novel imaging modalities can determine cartilage strain after physical activities^{48–50}, and computational models can be used to predict load-induced cartilage stresses and strains^{51,52}. With the appropriate load magnitudes and resultant physiological strains, controlled loading regimens could improve post-traumatic treatment of joints. For example, crutches and braces frequently are used to reduce weight-bearing following ACL injury⁵³. Reduced weight-bearing and unloading protect against DMM-induced post-traumatic OA progression⁵⁴. Here, low-magnitude loading overcame adverse stresses associated with habitual cage activity following DMM surgery. Combined, low-level loading could be even more effective in attenuating post-traumatic OA progression in the absence of habitual activity. Further research is necessary to determine the optimal timing and magnitude of post-traumatic loading to benefit the injured joint⁵⁵.

In conclusion, controlled low-level cyclic loading was beneficial to joint health and attenuated PTOA following DMM. Although protection was not observed in all regions of the knee joint, cartilage erosion, osteophyte formation, and subchondral bone sclerosis were attenuated. Low-level cyclic compression was equally as effective, if not more effective, in attenuating OA-like changes compared to similar non-invasive approaches. The beneficial effects were likely due to healthy tissue strains achieved by the low load magnitudes. Future work needs to focus on molecular events that result from low-level loading and translation to clinical use. In addition, although male mice develop PTOA rapidly and are used frequently in published studies involving the DMM model⁵⁶, future work needs to explore sex-dependent differences in the development and attenuation of PTOA by examining the effects of low-level loading in female mice. Ultimately, rehabilitation protocols following joint injury may benefit from controlled, low-level cyclic compression to maintain healthy cartilage and attenuate the development of PTOA.

Supplementary Material

Refer to Web version on PubMed Central for supplementary material.

Acknowledgments

We thank Drs. Christopher Hernandez, Mary Goldring, Mathias Bostrom, Scott Rodeo, Larry Bonassar, and Lisa Fortier for valuable input. We also thank Camila Carballo, Lyudmila Lukashova, and the Cornell CARE staff for experimental assistance. Funding was provided by NIH R21-AR064034, GAANN Fellowship (US Department of Education P200A150273), Robert and Helen Appel Fellowship, and the Clark and Kirby Foundations.

Role of the funding source

NIH R21-AR064034, GAANN Fellowship (US Department of Education P200A150273), Robert and Fielen Appel Fellowship, and the Clark and Kirby Foundations provided funding to support the collection, analysis, and interpretation of data. The sponsors had no role in the writing of the manuscript or in the decision to submit the manuscript for publication.

Competing interest statement

No author has any conflict of interest surrounding this work. Timothy Wright has grants/grant spending from Lima and Stryker, has royalties from Lima and Mathys, and owns stock in OrthoBond. Marjolein van der Meulen has grants/grants pending from NIH, NSF, and DOD, and is an associate editor for the Journal of Bone and Mineral Research.

References

- Lawrence RC, Felson DT, Helmick CG, Arnold LM, Choi H, Deyo RA, et al. Estimates of the prevalence of arthritis and other rheumatic conditions in the United States. Part II. *Arthritis Rheum.* 2008;58(1):26–35. [PubMed: 18163497]
- Turkiewicz A, Petersson IF, Björk J, Hawker G, Dahlberg LE, Lohmander LS, et al. Current and future impact of osteoarthritis on health care: a population-based study with projections to year 2032. *Osteoarthritis Cartilage.* 2014;22(11): 1826–1832. [PubMed: 25084132]
- Hootman JM, Helmick CG. Projections of US prevalence of arthritis and associated activity limitations. *Arthritis Rheum.* 2006;54(1):226–229. [PubMed: 16385518]
- Hunter DJ, Schofield D, Callander E. The individual and socioeconomic impact of osteoarthritis. *Nat Rev Rheumatol.* 2014; 10(7):437–441. [PubMed: 24662640]
- Kim HA, Blanco FJ. Cell death and apoptosis in osteoarthritic cartilage. *Curr Drug Targets.* 2007;8(2):333–345. [PubMed: 17305511]
- Mitchell PG, Magna HA, Reeves LM, Lopresti-Morrow LL, Yocum SA, Rosner PJ, et al. Cloning, expression, and type II collagenolytic activity of matrix metalloproteinase-13 from human osteoarthritic cartilage. *J Clin Invest.* 1996;97(3):761–768. [PubMed: 8609233]
- Nagase H, Kashiwagi M. Aggrecanases and cartilage matrix degradation. *Arthritis Res Ther.* 2003;5(2):94–103. [PubMed: 12718749]
- Brown TD, Johnston RC, Saltzman CL, Marsh JL, Buckwalter JA. Posttraumatic osteoarthritis: a first estimate of incidence, prevalence, and burden of disease. *J Orthop Trauma.* 2006;20(10):739–744. [PubMed: 17106388]
- Driban JB, Eaton CB, Lo GH, Ward RJ, Lu B, McAlindon TE. Association of knee injuries with accelerated knee osteoarthritis progression: data from the Osteoarthritis Initiative. *Arthritis Care Res (Hoboken).* 2014;66(11): 1673–1679. [PubMed: 24782446]
- Punzi L, Galozzi P, Luisetto R, Favero M, Ramonda R, Oliviero F, et al. Post-traumatic arthritis: overview on pathogenic mechanisms and role of inflammation. *RMD open.* 2016;2(2):e000279. [PubMed: 27651925]
- Felson DT. Risk Factors for Osteoarthritis. *Clin Orthop Relat Res.* 2004;427(427):S16–S21.
- Kurz B, Jin M, Patwari P, Cheng DM, Lark MW, Grodzinsky AJ. Biosynthetic response and mechanical properties of articular cartilage after injurious compression. *J Orthop Res.* 2001;19(6): 1140–1146. [PubMed: 11781016]
- Stolberg-Stolberg JA, Furman BD, William Garrigues N, Lee J, Pisetsky DS, Steams NA, et al. Effects of cartilage impact with and without fracture on chondrocyte viability and the release of inflammatory markers. *J Orthop Res.* 2013;31(8): 1283–1292. [PubMed: 23620164]

14. Christiansen BA, Anderson MJ, Lee CA, Williams JC, Yik JHN, Haudenschild DR. Musculoskeletal changes following non-invasive knee injury using a novel mouse model of post-traumatic osteoarthritis. *Osteoarthritis Cartilage*. 2012;20(7):773–782. [PubMed: 22531459]
15. Uthman OA, van der Windt DA, Jordan JL, Dziedzic KS, Healey EL, Peat GM, et al. Exercise for lower limb osteoarthritis: systematic review incorporating trial sequential analysis and network meta-analysis. *BMJ*. 2013;347:f5555. [PubMed: 24055922]
16. Sah RL-Y, Kim Y-J, Doong J-YH, Grodzinsky AJ, Plass AHK, Sandy JD. Biosynthetic response of cartilage explants to dynamic compression. *J Orthop Res*. 1989;7(5):619–636. [PubMed: 2760736]
17. Hubbard-Tumer T, Guderian S, Turner MJ. Lifelong physical activity and knee osteoarthritis development in mice. *Int J Rheum Dis*. 2015; 18(1):33–39. [PubMed: 24636482]
18. Galois L, Etienne S, Grossin L, Watrin-Pinzano A, Courmil-Henrionnet C, Loeuille D, et al. Dose-response relationship for exercise on severity of experimental osteoarthritis in rats: a pilot study. *Osteoarthritis Cartilage*. 2004;12(10):779–786. [PubMed: 15450527]
19. Hamamura K, Zhang P, Zhao L, Shim JW, Chen A, Dodge TR, et al. Knee loading reduces MMP13 activity in the mouse cartilage. *BMC Musculoskelet Disord*. 2013;14(1):312. [PubMed: 24180431]
20. Freeman PM, Natarajan RN, Kimura JH, Andriacchi TP. Chondrocyte cells respond mechanically to compressive loads. *J Orthop Res*. 1994; 12(3):311–320. [PubMed: 8207584]
21. Beckwée D, Vaes P, Cnudde M, Swinnen E, Bautmans I. Osteoarthritis of the knee: why does exercise work? A qualitative study of the literature. *Ageing Res Rev*. 2013; 12(1):226–236. [PubMed: 23026409]
22. Boveris A, Navarro A. Systemic and mitochondrial adaptive responses to moderate exercise in rodents. *Free Radic Biol Med*. 2008;44(2):224–229.
23. Poulet B, Hamilton RW, Shefelbine S, Pitsillides AA. Characterizing a novel and adjustable noninvasive murine joint loading model. *Arthritis Rheum*. 2011;63(1): 137–147. [PubMed: 20882669]
24. Ko FC, Dragomir C, Plumb DA, Goldring SR, Wright TM, Goldring MB, et al. In Vivo Cyclic Compression Causes Cartilage Degeneration and Subchondral Bone Changes in Mouse Tibiae. *Arthritis Rheum*. 2013;65(6): 1569–1578. [PubMed: 23436303]
25. Holyoak DT, Otero M, Armar NS, Ziemian SN, Otto A, Cullinane D, et al. Collagen XI mutation lowers susceptibility to load-induced cartilage damage in mice. *J Orthop Res*. 2017;36(2):711–720. [PubMed: 28898438]
26. Adebayo OO, Ko FC, Wan PT, Goldring SR, Goldring MB, Wright TM, et al. Role of subchondral bone properties and changes in development of load-induced osteoarthritis in mice. *Osteoarthritis Cartilage*. 2017;25(12):2108–2118. [PubMed: 28919430]
27. ISO 14243–1, Implants for Surgery Wear of Total Knee-Joint Prostheses—Part 1: Loading and Displacement Parameters for Wear-Testing Machines with Load Control and Corresponding Environmental Conditions for Test. ', 2009.
28. Glasson SS, Blanchet TJ, Morris EA. The surgical destabilization of the medial meniscus (DMM) model of osteoarthritis in the 129/SvEv mouse. *Osteoarthritis Cartilage*. 2007; 15(9): 1061–1069. [PubMed: 17470400]
29. Adebayo OO, Ko FC, Goldring SR, Goldring MB, Wright TM, van der Meulen MCH. Kinematics of meniscal- and ACL-transected mouse knees during controlled tibial compressive loading captured using roentgen stereophotogrammetry. *J Orthop Res*. 2017;35(2):353–360. [PubMed: 27153222]
30. Culley KL, Dragomir CL, Chang J, Wondimu EB, Coico J, Plumb DA, et al. Mouse Models of Osteoarthritis: Surgical Model of Posttraumatic Osteoarthritis Induced by Destabilization of the Medial Meniscus. In: Humana Press, New York, NY; 2015:143–173.
31. Kilkeny C, Browne WJ, Cuthill IC, Emerson M, Altman DG. Improving Bioscience Research Reporting: The ARRIVE Guidelines for Reporting Animal Research. *PLoS Biol*. 2010;8(6):e1000412. [PubMed: 20613859]
32. Fritton JC, Myers ER, Wright TM, Van Der Meulen MCH. Loading induces site-specific increases in mineral content assessed by microcomputed tomography of the mouse tibia. *Bone*. 2005;36(6): 1030–1038. [PubMed: 15878316]

33. Lynch ME, Main RP, Xu Q, Walsh DJ, Schäffler MB, Wright TM, et al. Cancellous bone adaptation to tibial compression is not sex dependent in growing mice. *J Appl Physiol*. 2010;109(3):685–691. [PubMed: 20576844]
34. Melville KM, Rohling AG, van der Meulen MCH. In vivo axial loading of the mouse tibia. *Methods Mol Biol*. 2015;1226:99–115. [PubMed: 25331046]
35. Glasson SS, Chambers MG, Van Den Berg WB, Little CB. The OARSI histopathology initiative - recommendations for histological assessments of osteoarthritis in the mouse. *Osteoarthritis Cartilage*. 2010; 18 Suppl 3:S17–23.
36. Little CB, Barai A, Burkhardt D, Smith SM, Fosang AJ, Werb Z, et al. Matrix metalloproteinase 13-deficient mice are resistant to osteoarthritic cartilage erosion but not chondrocyte hypertrophy or osteophyte development. *Arthritis Rheum*. 2009;60(12):3723–3733. [PubMed: 19950295]
37. Girish V, Vijayalakshmi A. Affordable image analysis using NIH Image/ImageJ. *Indian J Cancer*, 41(1):47. [PubMed: 15105580]
38. Varghese F, Bukhari AB, Malhotra R, De A. IHC Profiler: an open source plugin for the quantitative evaluation and automated scoring of immunohistochemistry images of human tissue samples. *PLoS One*. 2014;9(5):e96801. [PubMed: 24802416]
39. Stock M, Menges S, Eitzinger N, Geßlein M, Botschner R, Wormser L, et al. A Dual Role of Upper Zone of Growth Plate and Cartilage Matrix-Associated Protein in Human and Mouse Osteoarthritic Cartilage: Inhibition of Aggrecanases and Promotion of Bone Turnover. *Arthritis Rheumatol*. 2017;69(6):1233–1245. [PubMed: 28086000]
40. Lewis JS, Hembree WC, Furman BD, Tippets L, Cattel D, Huebner JL, et al. Acute joint pathology and synovial inflammation is associated with increased intra-articular fracture severity in the mouse knee. *Osteoarthritis Cartilage*. 2011;19(7):864–873. [PubMed: 21619936]
41. Donato S, Pacilè S, Colombo F, Garrovo C, Monego SD, Macor P, et al. Meniscal ossicles as micro-CT imaging biomarker in a rodent model of antigen-induced arthritis: Asynchrotron-based x-ray pilot study. *Sci Rep*. 2017;7(1): 1–7. [PubMed: 28127051]
42. Li X, Yang J, Liu D, Li J, Niu K, Feng S, et al. Knee loading inhibits osteoclast lineage in a mouse model of osteoarthritis. *Sci Rep*. 2016;6:24668. [PubMed: 27087498]
43. Zhang P, Sun Q, Turner CH, Yokota H. Knee loading accelerates bone healing in mice. *J Bone Miner Res*. 2007;22(12): 1979–1987. [PubMed: 17696761]
44. Iijima H, Aoyama T, Ito A, Yamaguchi S, Nagai M, Tajino J, et al. Effects of short-term gentle treadmill walking on subchondral bone in a rat model of instability-induced osteoarthritis. *Osteoarthritis Cartilage*. 2015;23:1563–1574. [PubMed: 25916553]
45. Allen J, Imbert I, Havelin J, Henderson T, Stevenson G, Liaw L, et al. Effects of Treadmill Exercise on Advanced Osteoarthritis Pain in Rats. *Arthritis Rheumatol*. 2017;69(7): 1407–1417. [PubMed: 28320059]
46. Sanchez-Adams J, Leddy HA, McNulty AL, O’Conor CJ, Guilak F. The mechanobiology of articular cartilage: bearing the burden of osteoarthritis. *Curr Rheumatol Rep*. 2014; 16(10):451. [PubMed: 25182679]
47. Poulet B, Westerhof TAT, Hamilton RW, Shefelbine SJ, Pitsillides AA. Spontaneous osteoarthritis in Str/ort mice is unlikely due to greater vulnerability to mechanical trauma. *Osteoarthritis Cartilage*. 2013;21(5):756–763. [PubMed: 23467034]
48. Lad NK, Liu B, Ganapathy PK, Utturkar GM, Sutter EG, Moorman CT, et al. Effect of normal gait on in vivo tibiofemoral cartilage strains. *J Biomech*. 2016;49(13):2870–2876. [PubMed: 27421206]
49. Cher WL, Utturkar GM, Spritzer CE, Nunley JA, DeFrate LE, Collins AT. An analysis of changes in in vivo cartilage thickness of the healthy ankle following dynamic activity. *J Biomech*. 2016;49(13):3026–3030. [PubMed: 27289415]
50. Halonen KS, Mononen ME, Jurvelin JS, Töyräs J, Salo J, Korhonen RK. Deformation of articular cartilage during static loading of a knee joint - Experimental and finite element analysis. *J Biomech*. 2014;47(10):2467–2474. [PubMed: 24813824]
51. Besier TF, Pal S, Draper CE, Fredericson M, Gold GE, Delp SL, et al. The role of cartilage stress in patellofemoral pain. *Med Sei Sport Exerc*. 2015;47(11):2416–2422.

52. Klets O, Mononen ME, Tanska P, Nieminen MT, Korhonen RK, Saarakkala S. Comparison of different material models of articular cartilage in 3D computational modeling of the knee: Data from the Osteoarthritis Initiative (OAI). *J Biomech.* 2016;49(16):3891–3900. [PubMed: 27825602]
53. Cavanaugh JT, Powers M. ACL Rehabilitation Progression: Where Are We Now? *Curr Rev Musculoskelet Med.* 2017;10(3):289–296. [PubMed: 28791612]
54. Burleigh A, Chanalaris A, Gardiner MD, Driscoll C, Boruc O, Saklatvala J, et al. Joint immobilization prevents murine osteoarthritis and reveals the highly mechanosensitive nature of protease expression in vivo. *Arthritis Rheum.* 2012;64(7):2278–2288. [PubMed: 22307759]
55. Bedi A, Kovacevic D, Fox AJ, Imhauser CW, Stasiak M, Packer J, et al. Effect of early and delayed mechanical loading on tendon-to-bone healing after anterior cruciate ligament reconstruction. *J Bone Jt Surg.* 2010;92(14):2387–2401.
56. Ma FI-L, Blanchet TJ, Peluso D, Flopkins B, Morris EA, Glasson SS. Osteoarthritis severity is sex dependent in a surgical mouse model. *Osteoarthritis Cartilage.* 2007;15(6):695–700. [PubMed: 17207643]

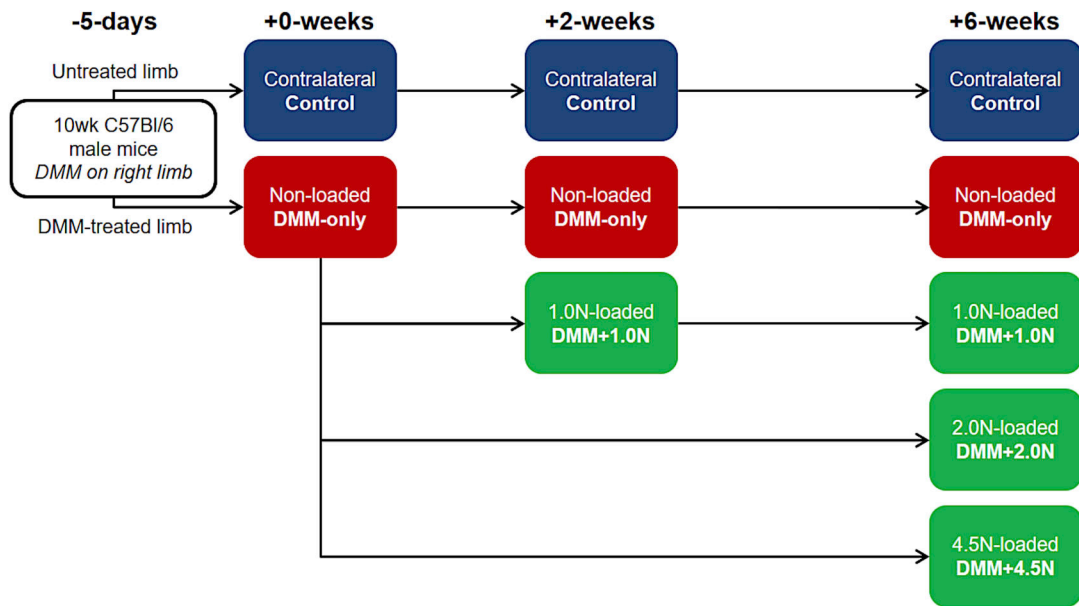


Figure 1. Experimental design. 10wk C57Bl/6 male mice underwent DMM surgery on their right limbs. Five days later (+0-weeks), DMM-operated limbs were either subjected to no loading (*DMM-only*), 1.0N-loading (*DMM+1.0N*), 2.0N-loading (*DMM+2.0N*), or 4.5N-loading (*DMM+4.5N*) for 2 or 6 weeks. Contralateral limbs served as controls at each time point. n=7–8 mice per group. Arrows connecting panels demonstrate the experimental design and are used in all figures with multiple timepoints.

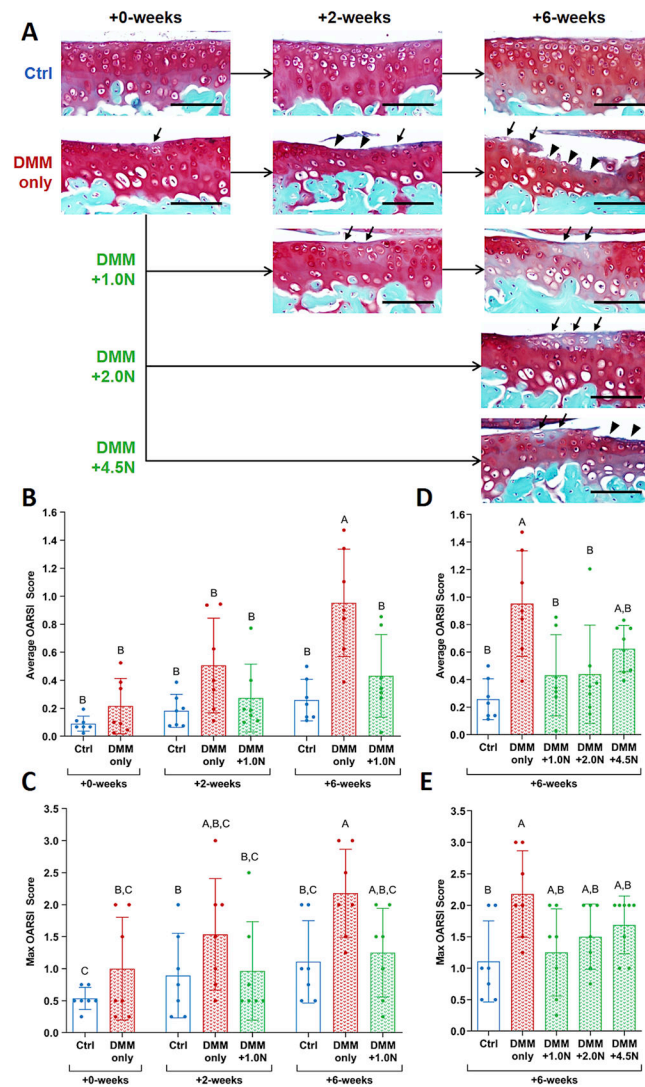


Figure 2. Low-level cyclic compression attenuated post-traumatic cartilage degradation. (A) Representative Safranin O/Fast Green histological images show that DMM surgery led to focal erosion extending to the tidemark in the medial tibial plateau in the *DMM-only* group. Loading at 1.0N attenuated DMM-induced cartilage erosion, evident from the intact cartilage surface. Loading at 2.0N had similar effects to 1.0N-loading, with an intact cartilage surface after 6 weeks. Moderate loading at 4.5N resulted in mild erosion and proteoglycan loss that was not different from *DMM-only*. (B) Average and (C) max OARSIS scores for cartilage damage were significantly different between the *DMM-only* vs. *DMM +1.0N* groups at +6-weeks. (D) 2.0N-loading also led to lower average OARSIS scores than *DMM-only*, (E) but not lower max OARSIS scores. Scale bars =100 μ m. Arrows indicate proteoglycan loss; arrow heads indicate erosion. Mean \pm SD shown with individual data points overlaid. Different letters between bars indicate significant differences in the means by two-factor ANOVA, followed by Tukey post-hoc tests ($p < 0.05$).

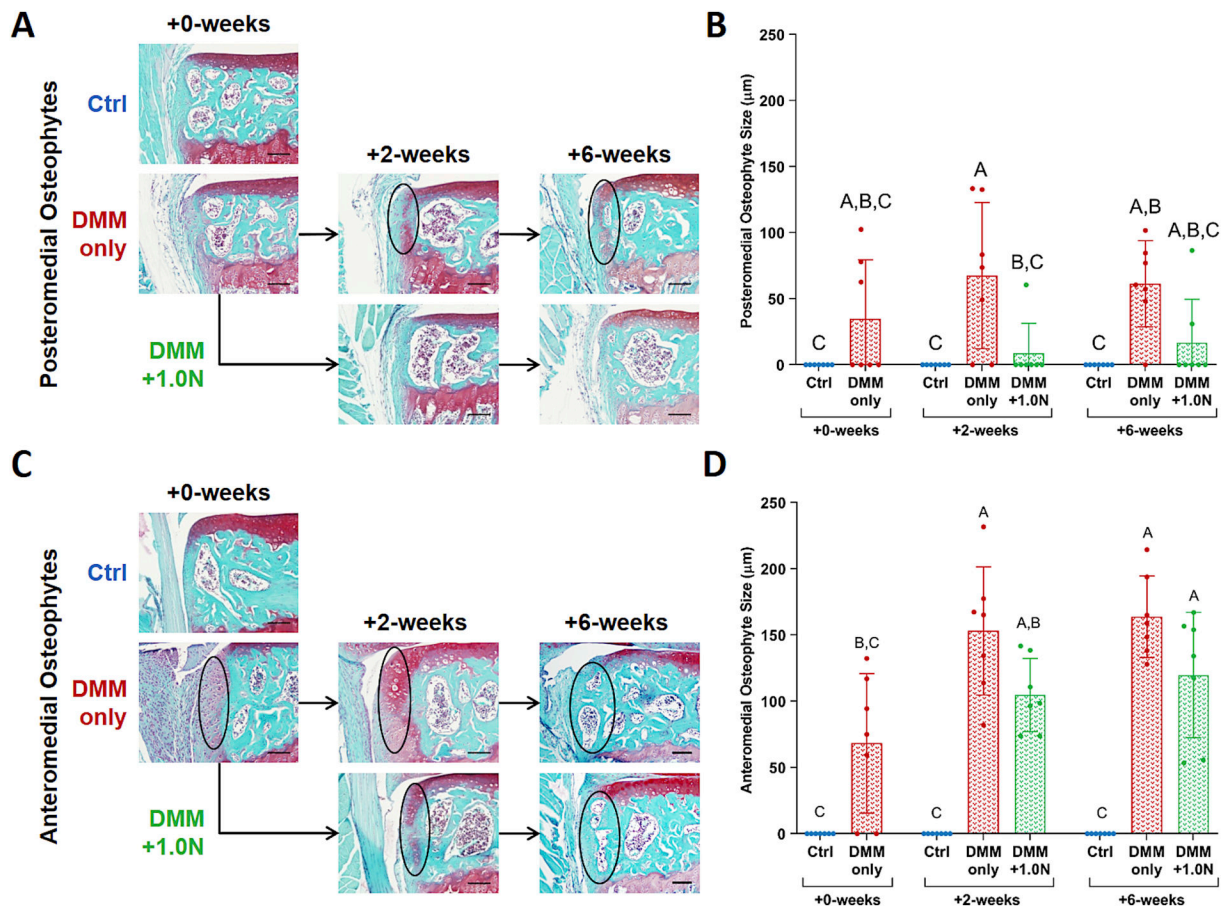


Figure 3. Low-level cyclic compression attenuated post-traumatic osteophyte formation. (A) Representative Safranin O/Fast Green histological images indicate that DMM surgery led to osteophyte formation on the anteromedial aspect of the tibial plateau as quickly as 5 days postsurgery. (B) Anteromedial osteophyte size increased in the *DMM-only* groups after 2 and 6 weeks, but was not different between the *DMM+1.0N* groups and +0-week *DMM-only* group (C) Low-level cyclic compression completely suppressed posteromedial osteophyte formation in nearly all animals. (D) Posteromedial osteophyte size in the *DMM +1.0N* group was lower compared to *DMM-only* groups. Scale bars =100 µm. Mean ± SD shown with individual data points overlaid. Different letters between bars indicate significant differences in the means by two-factor ANOVA, followed by Tukey post-hoc tests (p<0.05).

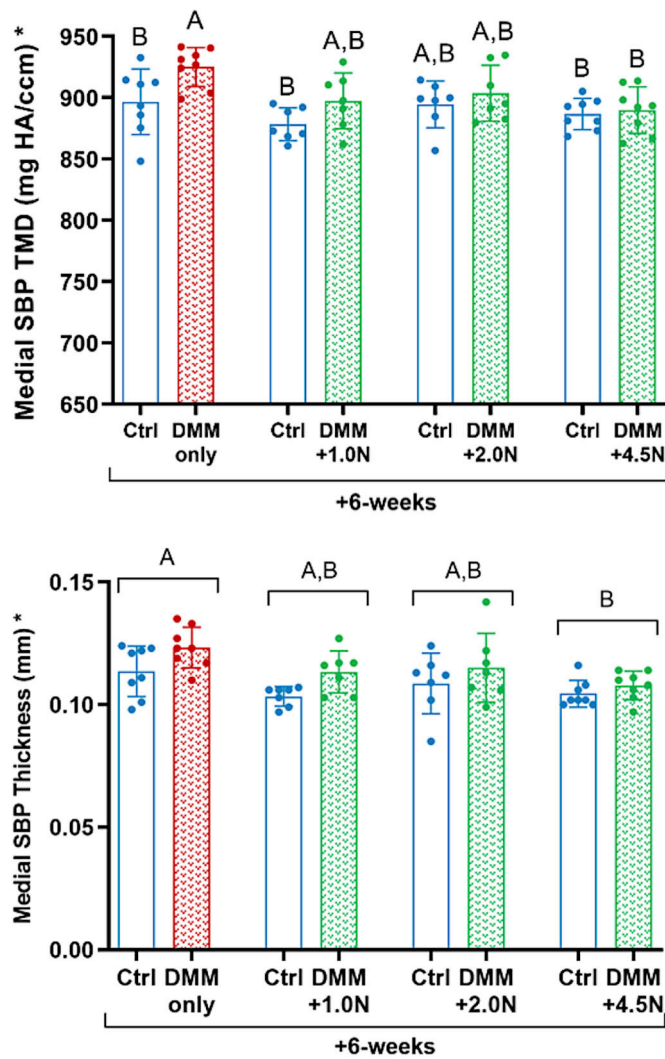


Figure 4. Low-level cyclic compression attenuated post-traumatic subchondral bone sclerosis. (A) At the +6-week time point, subchondral bone plate TMD increased in the medial tibial plateau in *DMM-only* limbs compared to contralateral control limbs. TMD was not different between control and operated limbs in the 1.0N-, 2.0N-, or 4.5N-loaded groups. (B) Mice in the *DMM-only* group had thicker medial subchondral cortical bone compared to mice in the moderate load group (*DMM+4.5N*). Mean \pm SD shown with individual data points overlaid. Different letters between bars or groups indicate significant differences in the means by two-factor ANOVA, followed by Tukey post-hoc tests ($p < 0.05$). Asterisk on y-axis title indicates significance by post-hoc comparisons for control vs. DMM-operated limbs.

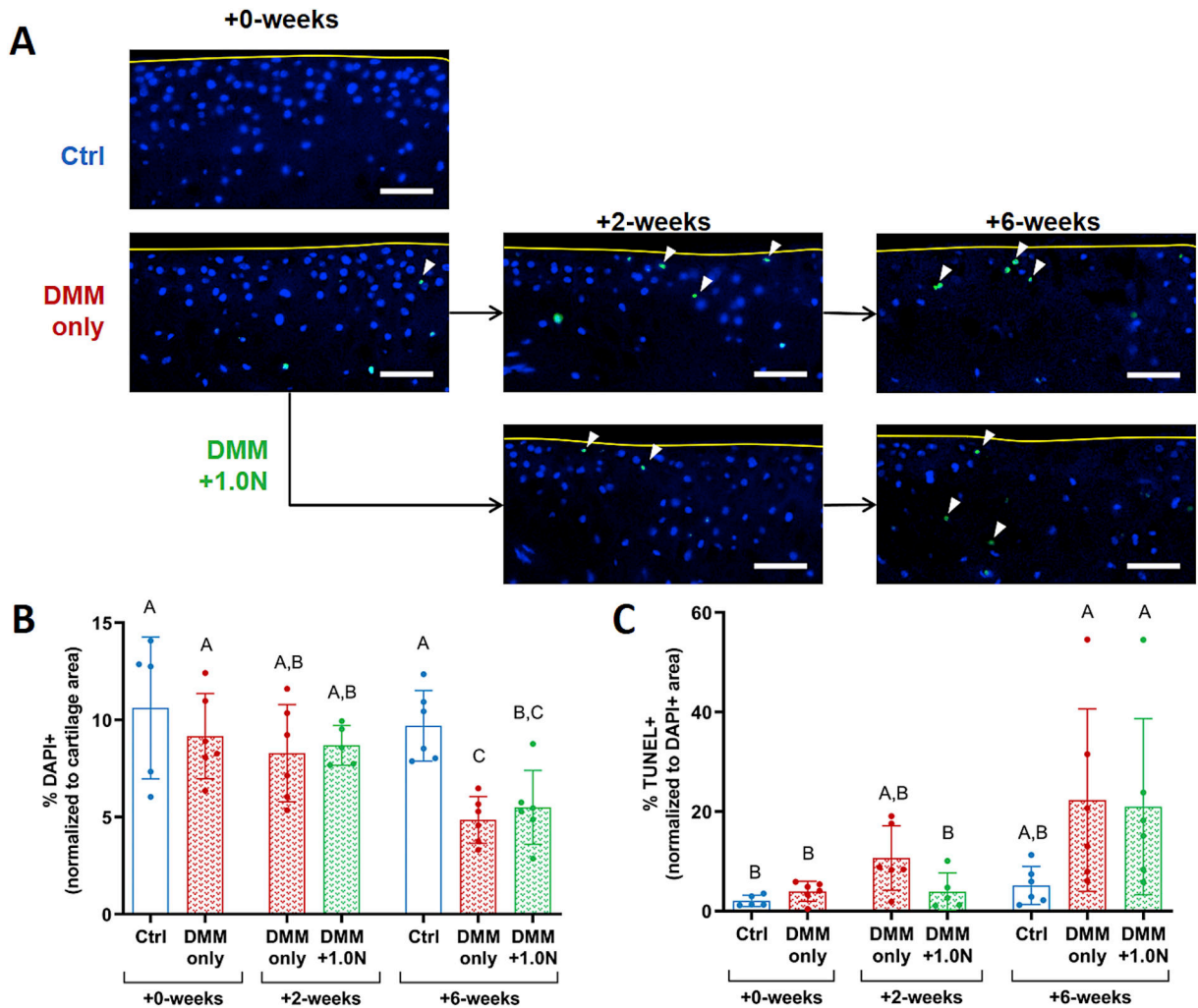


Figure 5.

Low-level cyclic compression had subtle beneficial effects on cellularity and apoptosis. (A) Representative DAPI (blue) overlaid with TUNEL (green) images show chondrocyte loss and apoptosis following DMM surgery, with the greatest degree of cell loss in the +6-week *DMM-only* group. (B) Cellularity decreased in the +6-week *DMM-only* group compared to the +2-week *DMM-only* limbs, whereas cellularity in the +6-week *DMM+1.0N* group was not different from the +2-week timepoint. However, cell loss was not different between the *DMM-only* and *DMM+1.0N* groups at the +2-week and +6-week time points. (C) Chondrocyte apoptosis increased after DMM surgery. At +2-weeks, apoptosis levels in the *DMM-only* group were not different from +6-week levels, whereas the increase in apoptosis in the *DMM+1.0N* group was delayed. However, chondrocyte apoptosis was not different between the *DMM-only* and *DMM+1.0N* groups at the +2-week and +6-week time points. Scale bars = 100 pm. Arrow heads denote apoptotic cells. Yellow curves designate tibial cartilage surface. Mean \pm SD shown with individual data points overlaid. Different letters between bars indicate significant differences in the means by one-factor ANOVA, followed by Tukey post-hoc tests ($p < 0.05$).

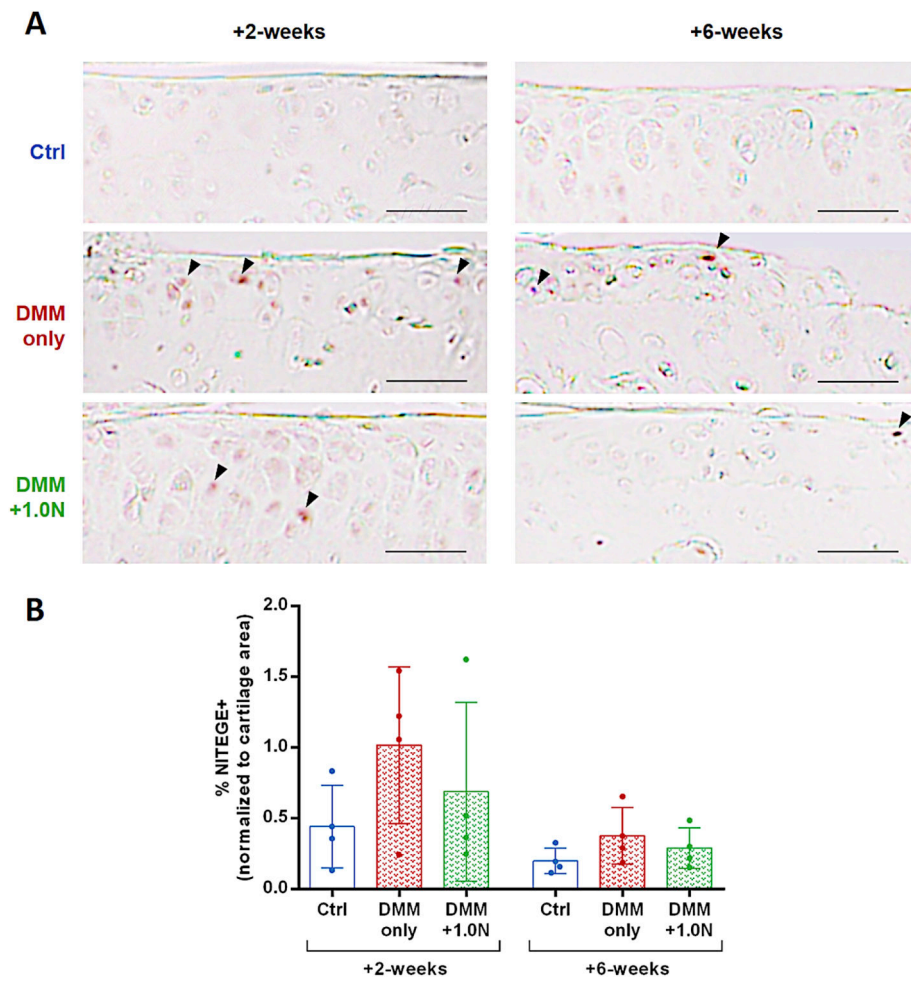


Figure 6. Low-level cyclic compression had subtle beneficial effects on aggrecanase activity. (A) Representative IHC images show NITEGE immunostaining in control, *DMM-only*, and *DMM+1.0N* at the +2-week and +6-week time point, with the highest levels of positive immunostaining in the *DMM-only* group. (B) Aggrecanase activity was 116% higher in *DMM-only* limbs compared to control limbs, and only 53% higher in *DMM+1.0N* limbs compared to controls. However, these changes were not significant due to small sample size. Scale bars =100 pm. Arrow heads indicate positive signal. Mean \pm SD shown with individual data points overlaid.